DOI: https://doi.org/10.34123/jurnalasks.v16i2.732

POLITEKNIK STATISTIKA STIS

Jurnal Aplikasi Statistika & Komputasi Statistik
Vol. 16 No. 2 December 2024
*e- ISSN: 2615-1367, p-ISSN:2086-4132*

Available online at https://jurnal.stis.ac.id/

# The Utilization of Model Output Statistic (MOS) in Improving Weather Prediction Model Accuracy of Integrated Forecasting System (IFS)

**Isnaini Anjelina Ramadhan[1*], Deni Septiadi [2]**

*[1,2]State College of Meteorology Climatology and Geophysics, Tangerang, Indonesia*
**Corresponding Author: E-mail address:* isnainianjelinar@gmail.com

## ARTICLE INFO

***Article history:***
Received 11 March, 2024
Revised 20 April, 2024
Accepted 7 May, 2024
Published 31 December, 2024

***Keywords:***
Accuracy; IFS; MOS; Prediction; Regression; Weather

## Abstract

**Introduction/Main Objectives:** Integrated Forecasting System (IFS) is one of the most accurate numerical weather prediction (NWP) model for Indonesia region. **Background Problems:** However, in fact, each model always has bias potential against observation which causes inaccuracy in weather prediction. **Novelty:** This research intends to overcome this problem by building a weather prediction model based on Model Output Statistic (MOS) to minimize bias and improve NWP accuracy. **Research Methods:** Provide an outline of the research method(s) and data used in this paper. Explain how did you go about doing this research. Again, avoid unnecessary content and do not make any speculation(s). **Finding/Results:** Analysis result states that compared to IFS, MOS fluctuation pattern is more relevant to observation. MOS has higher correlation to observation and lower error. However, the variance of observation value tends to be better represented by IFS. The test result of heavy rain cases prove that the application of MOS is able to provide fairly accurate prediction. This weather prediction will be able to be the basis for decision-making and preventive measure in dealing with extreme condition that may occur.

## 1. Introduction

Weather prediction is one of the crucial needs to support the smooth operation of the public sector. According to *Badan Nasional Penanggulangan Bencana (BNPB) or National Disaster Management Agency* [1], in 2022 there is 3,544 natural disasters that hit Indonesia. As many as 99.2% of events is dominated by hydrometeorological disasters. Flooding is the disaster with the highest frequency at 1,531 events, followed by extreme weather at 1,068 events. These disasters are closely related to meteorological condition. Therefore, weather prediction is important for decision-making and preventive measures in dealing with extreme condition that may occur [2].

*Badan Meteorologi Klimatologi dan Geofisika* (BMKG) or Meteorology Climatology and Geophysics Agency, as a weather service provider in Indonesia, applies numerical weather prediction (NWP) method in making weather prediction. The model used by BMKG is integrated in the workstation named 'Synergie' which contains four models, including the Global Forecast System (GFS), Integrated Forecasting System (IFS), ARPEGE, and Weather Research and Forecasting (WRF). The model that has the best performance so far is IFS. According to Kiki and Alam [3], IFS is proved to be able to predict 24-hour accumulated precipitation in various classifications, including per year, per month, per season, per province, to the average percentage per month better than the other three models mentioned.

However, it should be noted that every weather model has the potential to produce bias against observation. The input of observation and assimilation data has the potential to cause uncertainty in the estimation of atmospheric condition [4]. Therefore, a processing method is needed to optimize the work of weather prediction model.

The optimization of NWP can be done by statistical post-processing method, one of which is through model output statistic (MOS). MOS is a method that relates between weather observation as predictand and NWP parameter as predictor using regression model [5] [6]. The first MOS research is developed by National Weather Service (NWS) Oceanic and Atmospheric Administration (NOAA) which is published through the research of Glahn and Lowry [5]. Brunet et al. [7] also conducts research to compare the results of perfect-prog (PP) prediction with MOS prediction. The result is that PP prediction tends to be more suitable for short-term prediction and more sensitive in displaying extreme weather. In contrast, MOS is more suitable for longer period and more reliable because it can overcome model limitation. The German meteorological agency, Deutscher Wetterdienst (DWD), also claims that MOS has high weather prediction accuracy [8]. In operational, DWD launches a MOS-based weather forecast product that combines the Integrated Forecasting System (IFS) and Icosahedral Nonhydrostatic (ICON) models, which is named MOSMIX.

Based on these superiorities, this research intends to build MOS-based weather prediction to improve the accuracy of IFS model. Predicted parameters include temperature, relative humidity, and QFF pressure. MOS will be tested to predict the weather in several cases of rain that had occurred in DKI Jakarta. Three cases of heavy rain (intensity > 50 mm/day) during January to February 2023 has been selected as samples, including January 1, 2023; January 4, 2023; and February 24, 2023. This research is relatively new because the application of MOS in Indonesia is still minimum. The application of MOS to the IFS model has been carried out by DWD with research location in Europe, especially Germany [8]. However, the use of IFS in several MOS studies in Indonesia [6] [9] [10] has not been found yet. Hence, through this research, the application of MOS to IFS for weather prediction in Indonesia is a new matter.

The regression model used to build MOS prediction is stepwise regression with forward selection type. The reason for this selection is because stepwise regression can select predictors with the highest correlation to be included in the model equation. Stepwise regression has been used in making MOS predictions at NWS based on the research of Glahn and Lowry [5] and has been proofed to improve NWP result. Although the predictand is correlated with hundreds of predictors, a regression equation containing only a few predictors can also approximate the observation. An equation that contains too many predictors have the potential to produce worse prediction. Other studies that also utilize stepwise regression in building MOS prediction include Bocchieri et al. [11], Klein and Glahn [12], and Kuligowski and Barros [13].

The location selection of DKI Jakarta is based on the vulnerability that may be obtained when a disaster occurs. According to Badan Penanggulangan Bencana Daerah (BPBD) or Local Disaster Management Agency of DKI Jakarta [14], in 2021 there are 375 hydrometeorological disaster events including floods, strong winds, fallen trees, landslides, and flooded roads. Based on this number, there are 75 floods that affected 51,294 people in 118 sub-districts. As for the 12 landslide incidents, the losses are estimated at 420 million rupiah. In addition, Indonesia's multi-sectoral activities are centered in DKI Jakarta. DKI Jakarta is a fairly dense province with a projected population of 10,679,951 in 2022 [15]. This target is expected to get benefits form this research. This effort to improve the accuracy of IFS are expected to provide positive results in starting the step of accurate objective weather prediction service.

The purpose of this research is to utilize MOS to minimize the bias produced by prediction against observation. This research intends to analyze the most suitable MOS regression model for weather prediction, analyze the performance test between IFS and MOS prediction against observation, and analyze the ability of MOS predictions of heavy rain cases in DKI Jakarta.

## 2. Material and Methods

### *2.1. Literature Review*

#### *2.1.1. Model Output Statistic (MOS)*

Model output statistic (MOS) is an objective weather prediction method expressed by statistical relationship between predictors and predictands using numerical method at a certain time projection [5]. This method utilizes weather observation as a predictand and NWP output as a predictor based on regression [9] [10]. In general, the function of MOS can be written in the following equation.

$$\hat{y}_t = f_{MOS}(x_t)$$

Description:
$\hat{y}_t$ : weather forecast at time t
$x_t$ : NWP output variable at time t

### *2.1.2. Numerical Weather Prediction (NWP)*

Numerical weather prediction (NWP) is a system of equations that describes the essential physical rules governing motion and processes in the atmosphere [16]. NWP calculation basically uses partial integral equation. There are three components that need to be taken into account, including observation, diagnostic or analysis, and prognostic [17].

Palmer [18] mentions that there are three uncertainties that cause NWP to deviate and cause bias, including initial uncertainty, model uncertainty, and external parameter uncertainty.

### *2.1.3. Integrated Forecasting System (IFS)*

The Integrated Forecasting System (IFS) is NWP model developed by the European Center for Medium-Range Weather Forecast (ECMWF) in collaboration with Météo-France. IFS is obtained by applying the semi-implicit semi-Lagrangian (SL) method to solve dynamic equations [19]. Currently, NWP calculations are performed by supercomputers that simultaneously predict weather. IFS routinely performs data assimilation by adding the latest observational data to produce model output [20]. These include atmospheric, oceanic, and physical land surface parameters [21].

IFS is a global model that includes surface level and elevation data for all regions on Earth. There are two types of IFS models, namely high-resolution forecasts (HRES) and ensemble forecasts (ENS) [22]. HRES is a single-forecast model consisting of only one model configuration. Meanwhile, ENS is an ensemble model that consists of several model combinations. This research will focus on single-forecast HRES.

### *2.1.4. Stepwise Regression*

Stepwise regression or screening regression is a regression model that uses independent variables as a reference for model processing result. This research uses the forward selection type. According to Glahn and Lowry [5], as well as Kuligowski and Barros [13], the first step in this procedure is to select the variable that is most highly correlated with the prediction (either positive or negative). Next, selecting the variable that together with the first variable increases the reduction of the highest variance. Selection can continue in this way until cut off criterion based on p-value is met. The requirement for a variable to enter the model is that the p-value must be less than α.

## *2.2. Location and Time Research*

The research location focuses on province of DKI Jakarta. In this location there are three meteorological stations, namely Tanjung Priok Maritime Meteorological Station, Kemayoran Meteorological Station, and Halim Perdana Kusuma Meteorological Station. The three were chosen in order to represent the distribution of observation locations as shown in Figure 1.

The research focuses from January 2022 to February 2023. The year 2022 is used as training period, while the year 2023 as testing period. In the testing period, three cases of heavy rain (intensity > 50 mm/day) that hit DKI Jakarta is selected, for instances January 1, 2023; January 4, 2023; and February 24, 2023. The amount of rainfall is presented in Table 1.

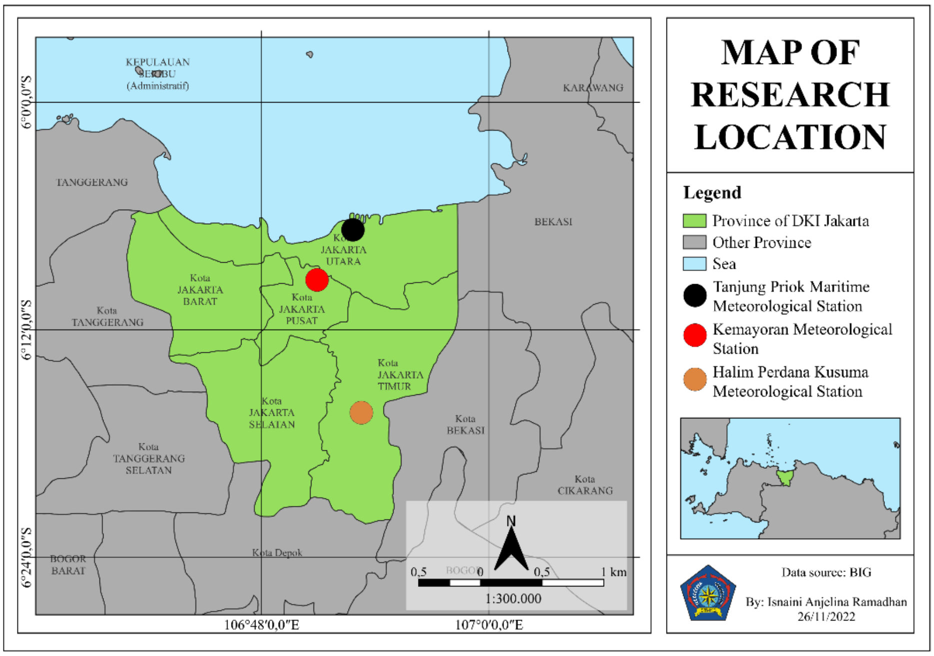


**Figure 1.** Map of research location.

**Table 1.** Sample cases of heavy rain in DKI Jakarta during January to February 2023

| Date | Rainfall (mm) | | |
|---|---|---|---|
| | Tanjung Priok | Kemayoran | Halim Perdana Kusuma |
| January 1, 2023 | 134.4 | 31.5 | 6.9 |
| January 4, 2023 | 31.3 | 35.3 | 79.6 |
| February, 24 2023 | 54.7 | 69.0 | 84.0 |

Source: BMKG (2023)

## 2.3. Data

### 2.3.1. IFS Data

The IFS data used in this study is HRES which is a single-forecast model. HRES data has spatial resolution of 0.08° x 0.08° or 9 km x 9 km [23]. The temporal resolution is 3 hours with a cycle every 12 hours at 00 and 12 UTC. This research uses single level forecast data consisting of 44 single level and pressure level meteorological parameters.

### 2.3.2. Synoptic Observation Data

Synoptic observation data is obtained from weather observation at the meteorological station tool park. The measurement tool used is a conventional tool. The data used includes air temperature, relative humidity, and QFF pressure with a range of every three hours. The selection of these parameters is because they are the basic weather parameters that are always observed every hour so that their fluctuations can be observed in detail (in this study a three-hour time span is used to adjust the temporal resolution of IFS).

## 2.4. Flowchart

The research steps in a coherent and structured manner are presented in Figure 2. Based on the flowchart, more detailed explanation of the research steps is as follows.

1. Performing pre-processing step, including:
   a. Extracting IFS model data from GRIB file into CSV format.
   b. Managing missing data using curve fitting method

c. Performing stationary test using correlogram based on autocorrelation (ACF) and partial autocorrelation (PACF) values. ACF is the correlation or relationship of a time series data for different lags. The ACF value can be obtained using the following equation [24].

$$\rho_k = \frac{\gamma_k}{\gamma_0} = \frac{cov(z_t, z_{t+k})}{\sqrt{Var(z_t)}\sqrt{Var(z_{t+k})}} \quad (1)$$

Description:
$\rho_k$ : ACF function at lag k
$\gamma_k$ : auto covariance of $z_t$ and $z_{t+k}$
$t$ : time
$Var(z_t)$ : constant variance
The value of the PACF function is the development of the ACF by removing linear dependencies on the variables of $Zt$+1, $Zt$+2, dan $Zt$+$k$-1

d. Performing data normalization to homogenize the data range according to the following equation.

$$x_{norm} = \frac{x - x_{min}}{x_{maks} - x_{min}} \quad (2)$$

2. Dividing the data into two groups, as training data and testing data. The training data is from January to December 2022, while the testing data is from January to February 2023.
3. Building MOS prediction using stepwise regression. The cut off criteria for the selection of predictors is limited to p-value 0,05. If a parameter has $\alpha < 0.05$, it is considered to be included in the regression model. This process produces a regression equation that becomes the basis for building MOS prediction.
4. Calculating MOS weather prediction for testing period derived from the calculation of IFS model data by regression equation. The results then go through denormalization process to restore the actual value of weather parameters.
5. Testing the performance of IFS and MOS prediction against observation data for the group of testing data. The performance tests include graph analysis and Taylor diagram. Verification uses several calculations, including:
   a. Correlation coefficient (r)

$$r = \frac{\sum_{i=1}^{N}(F_i - \bar{F})(O_i - \bar{O})}{\sqrt{\sum_{i=1}^{N}(F_i - \bar{F})^2 \cdot \sum_{i=1}^{N}(O_i - \bar{O})^2}} \quad (3)$$

Description:
$F_i$ : predicted value
$\bar{F}$ : average prediction
$O_i$ : observation value
$\bar{O}$ : average observation
$N$ : number of data

The value of correlation coefficient is interpreted in the following categories.

**Table 2.** Correlation coefficient interpretation

| Value of Correlation Coefficient | Interpretation |
|---|---|
| < 0,20 | Data relationship is considered non-existent |
| 0,20—0,40 | Low relationship |
| >0,40—0,70 | Moderate relationship |
| >0,70—0,90 | High relationship |
| >0,90—1,00 | Very high relationship |

Source: Sarwono, 2006

b. Root mean square error (RMSE)

$$RMSE = \sqrt{\frac{1}{N}\sum_{i=1}^{N}(F - O)^2} \tag{4}$$

c. Standard deviation

$$s = \sqrt{\frac{\sum_{i=1}^{N}(x_i - \bar{x})^2}{N-1}} \tag{5}$$

6. Conducting cases test on three heavy rain events. The MOS prediction results for each case were compared with the observed value and residual.

$$Residual = F - O \tag{6}$$

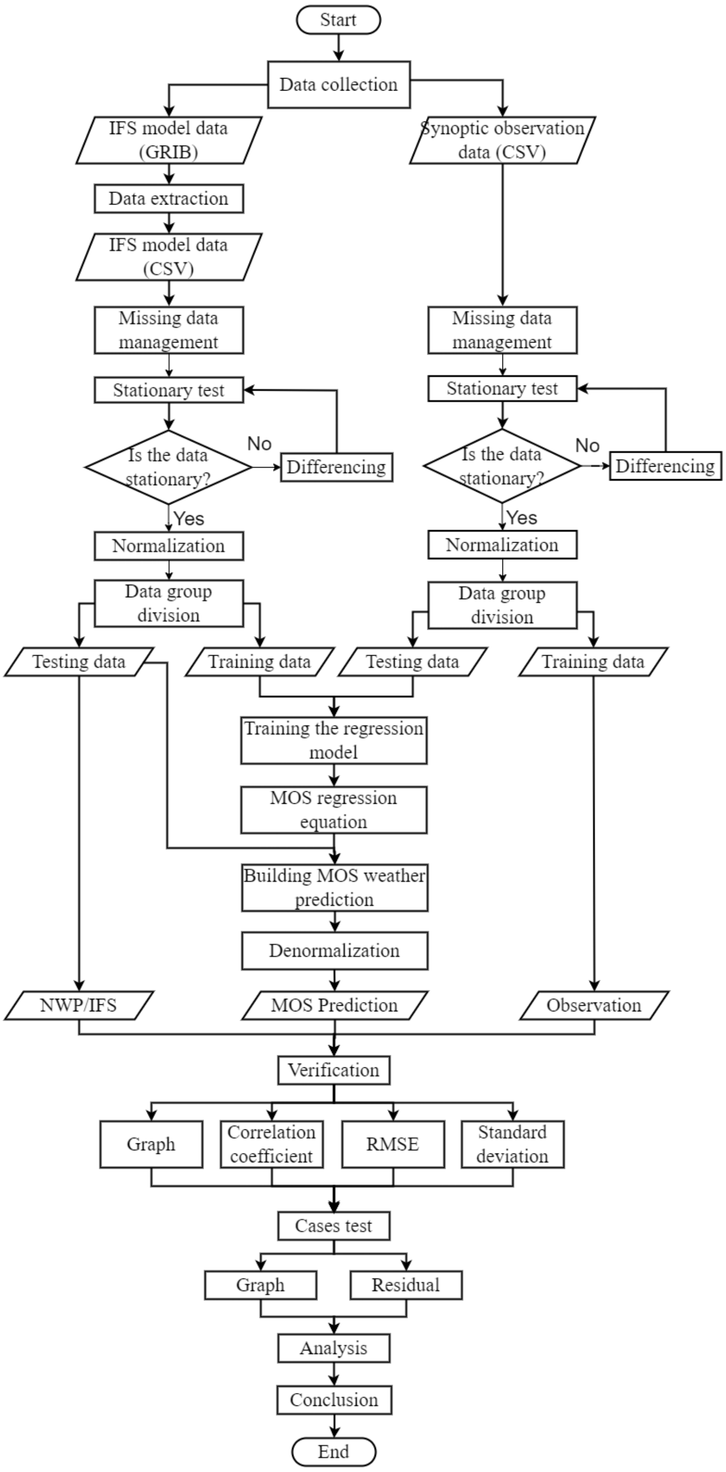


**Figure 2.** Research flowchart

## 3. Result and Discussion

### *3.1. Regression Configuration of Model Output Statistic (MOS)*

### *3.1.1. Air Temperature*

Table 3 shows the regression configuration for air temperature at Tanjung Priok. The adjusted R-squared value is 0.730, which means that 73.0% of the independent variables can explain the dependent variable. Parameter 2t (surface temperature) is the most influential variable with the highest coefficient value among others, which is 0.517.

**Table 3.** Configuration of MOS regression for air temperature at Tanjung Priok

| Variable | Coefficient |
|---|---|
| 2t | 0.517333 |
| C | 0.223572 |
| papt1000 | -0.190083 |
| Msl | -0.210207 |
| r925 | 0.088743 |
| w500 | -0.103157 |
| t1000 | 0.260527 |
| w1000 | 0.111158 |
| v10 | -0.210126 |
| t200 | 0.055796 |
| r500 | 0.075744 |
| Tp | 0.185290 |
| w700 | -0.069637 |
| r1000 | 0.050890 |
| v1000 | 0.142059 |
| t0 | -0.054935 |

Next, the configuration of MOS regression for air temperature at Kemayoran is described Table 4. The adjusted R-squared value is 0.738, which is 73.8% of the independent variables can explain the dependent variable.  Almost the same as Tanjung Priok, parameter 2t is the variable that mostly affects the temperature with the highest coefficient value, which is 0.638.

**Table 4.** Configuration of MOS regression for air temperature at Kemayoran

| Variable | Coefficient |
|---|---|
| 2t | 0.637556 |
| Tp | 0.238667 |
| Sp | -0.131850 |
| papt1000 | -0.110720 |
| r925 | 0.119823 |
| papt200 | 0.043699 |
| w1000 | 0.113805 |
| v10 | -0.281386 |
| t1000 | 0.146022 |
| v1000 | 0.204717 |
| w700 | -0.089568 |
| r500 | 0.072898 |
| u700 | 0.057743 |
| t850 | 0.045713 |
| t200 | 0.040517 |
| v500 | -0.048726 |

Furthermore, Table 5 shows the configuration of MOS regression for air temperature at Halim Perdana Kusuma. The adjusted R-squared value is 0.735, which means 73.5% of the independent variables can explain the dependent variable. Again, parameter 2t is the parameter that mostly affects the observed temperature that the coefficient value is 0.641.

**Table 5.** Configuration of MOS regression for air temperature at Halim Perdana Kusuma

| Variable | Coefficient |
|---|---|
| 2t | 0.641155 |
| t1000 | 0.295131 |
| tp | 0.227148 |
| v10 | -0.149102 |
| t925 | -0.110649 |
| papt1000 | -0.113882 |
| w1000 | 0.273773 |
| sp | -0.069180 |
| w925 | -0.093330 |

| Variable | Coefficient |
|---|---|
| t200 | 0.047487 |
| u700 | 0.075918 |
| papt850 | 0.077945 |

Overall, the dependent variable can be explained by 73.0% to 73.8% of the independent variables. Parameter 2t is the parameter that has the greatest influence in producing MOS temperature prediction. This is because parameter 2t is actually an IFS model for surface temperature at 2 meters in height.

### 3.1.2. Relative Humidity

Table 6 shows the configuration of MOS regression for relative humidity at Tanjung Priok. The adjusted R-squared is 0.644, it means that 64.4% of the independent variables can explain the dependent variable. Parameter 2t (surface temperature) is the parameter that mostly affects the relative humidity of Tanjung Priok, that is proved by the largest coefficient value among others, which is -0.633. Negative value has an effect by reducing the predicted value so that it is more appropriate with the observation.

**Table 6.** Configuration of MOS regression for relative humidity at Tanjung Priok

| Variable | Coefficient |
|---|---|
| c | 0.415155 |
| 2t | -0.632871 |
| r1000 | 0.329955 |
| w1000 | -0.189518 |
| msl | 0.250727 |
| t925 | 0.101252 |
| t1000 | 0.200183 |
| papt1000 | 0.074940 |
| w500 | 0.100016 |
| v850 | 0.041084 |
| t0 | 0.056962 |
| u500 | -0.055033 |
| r200 | -0.029158 |

**Table 7.** Configuration of MOS regression for relative humidity at Kemayoran

| Variable | Coefficient |
|---|---|
| r1000 | 0.365408 |
| msl | 0.183062 |
| r2 | 0.040282 |
| 2t | -0.571388 |
| c | 0.527001 |
| t1000 | 0.268587 |
| w1000 | -0.120337 |
| r925 | -0.085770 |
| u700 | -0.053809 |
| r500 | -0.057680 |
| w500 | 0.065190 |

The configuration of MOS regression for relative humidity at Kemayoran is explained in Table 7. Adjusted R-squared value is 0.648, it explains that 64.8% of the independent variables are able to explain the dependent variable. Among the other parameters, parameter 2t has the largest coefficient value, which is -0.571. Just like MOS prediction for relative humidity at Tanjung Priok, parameter 2t also has negative coefficient that reduce the predicted value.

Next, **Error! Not a valid bookmark self-reference.** explains the MOS configuration for relative humidity at Halim Perdana Kusuma. The adjusted R-squared value is 0.675, which means that 67.5% of the independent variables can explain the dependent variable. Parameter 2t is the parameter with the highest coefficient of -0.464. Similar to the previous two locations, the negative coefficient has an influence by providing reduction in value so that the MOS prediction becomes more appropriate.

**Table 8.** Configuration of MOS regression for relative humidity at Halim Perdana Kusuma

| Variable | Coefficient |
|---|---|
| r1000 | 0.330640 |
| t925 | 0.087774 |
| 2t | -0.464465 |
| C | 0.736266 |
| Sp | 0.081185 |
| papt1000 | 0.082203 |
| Tp | -0.123675 |
| papt700 | -0.082258 |
| w1000 | -0.265422 |
| v1000 | 0.107520 |
| w925 | 0.078613 |
| u700 | -0.078555 |

Overall, the dependent variable can be explained by 64.4% to 67.5% of the independent variables. Regressions at the three locations show that the most influential parameter on the MOS relative humidity prediction is parameter 2t (surface temperature) or temperature at 2 meters in height. This is because temperature and relative humidity are interrelated. Higher air temperature will cause water vapor composition in the air to increase, so relative humidity also increases. Practically, relative humidity is calculated through equations: $RH = 100 - 5(T_{BK} - T_d)$ or $RH = 100 - 7(T_{BK} - T_{BB})$. Relative humidity (RH) is obtained from temperature measurement of the dry bulb thermometer $(T_{BK})$, wet bulb thermometer $(T_{BB})$, and dew point $(T_d)$. Temperature of dry bulb thermometer $(T_{BK})$ is another name for the measurement of air temperature at height of 2 meters. Therefore, it is understandable that parameter 2t provides the largest regression coefficient for predicting relative humidity.

Besides that, parameter r1000 (relative humidity at 1000 mb) is the most influential variable after parameter 2t. The 1000 mb altitude is considered as the near-surface geopotential altitude (sea level pressure measurement). Although the definition of relative humidity observation in operational is different from the measurement at 1000 mb, this value is quite representative to surface relative humidity.

### *3.1.3. QFF Pressure*

Table 9 shows the configuration of MOS regression at Tanjung Priok. The adjusted R-squared value is 0.845, it states that 84.5% of the independent variables can explain the dependent variable. The greatest predictive influence is determined by msl (mean sea level pressure) with coefficient of 2.549.

The MOS configuration at Kemayoran for QFF pressure is shown in Table 10. The adjusted R-squared value is 0.905. Hence, 90.5% of the independent variables are able to explain the dependent variable. So far, this value is the highest among the three locations and other parameters. Similar to Tanjung Priok, msl is the most influential parameter on QFF pressure, which is 2.653.

Furthermore, Table 11 shows the configuration of MOS regression for QFF Pressure at Halim Perdana Kusuma. The adjusted R-squared value is 0.508, which means that 50.8% of the independent variables can explain the dependent variable. This number is not good enough to prove the performance of the training data, because it means that 49.1% of the independent variables fail to explain the dependent variable. This value is lower than the other two locations. Meanwhile, the parameter that is most influential to the regression is msl, its coefficient is 0.261.

**Table 9.** Configuration of MOS regression for QFF pressure at Tanjung Priok

| Variable | Coefficient |
|---|---|
| Sp | -0.586013 |
| C | -0.405385 |
| msl | 2.549298 |
| t0 | -0.180187 |
| t925 | 0.075094 |
| t200 | -0.060315 |
| papt1000 | 0.088071 |
| t850 | 0.053665 |

| Variable | Coefficient |
|---|---|
| r500 | -0.067441 |
| t700 | 0.035540 |
| v1000 | 0.125643 |
| v10 | -0.105918 |
| u925 | -0.031156 |
| u700 | -0.030579 |
| v500 | -0.041657 |
| w925 | -0.038344 |

**Table 10.** Configuration of MOS regression for QFF pressure at Kemayoran

| Variable | Coefficient |
|---|---|
| Sp | -0.476642 |
| C | -0.850700 |
| msl | 2.652981 |
| t925 | 0.165593 |
| t700 | 0.107852 |
| t0 | -0.056510 |
| t500 | 0.058274 |
| 2t | -0.139103 |
| t1000 | 0.058935 |
| papt1000 | 0.058935 |
| papt925 | 0.055624 |
| t850 | 0.031138 |
| u925 | -0.027976 |
| v500 | -0.033466 |
| w200 | -0.053179 |
| w500 | 0.055966 |
| r700 | 0.035132 |

**Table 11.** Configuration of MOS regression for QFF pressure at Halim Perdana Kusuma

| Variable | Coefficient |
|---|---|
| c | 0.317989 |
| msl | 0.260788 |
| 2t | -0.116825 |
| papt1000 | 0.080734 |
| t1000 | 0.086738 |
| t925 | 0.037626 |
| t200 | -0.031259 |
| u200 | -0.035565 |
| v700 | -0.035796 |
| u1000 | 0.026117 |
| tp | -0.055914 |
| v500 | -0.037715 |

For QFF pressure prediction, the dependent variable can be explained by 50.8% to 90.5% independent variables. These ranges are the lowest and highest values in this research. In all three locations, msl (mean sea level) has the largest regression coefficient value. Therefore, this parameter is the most influential in predicting QFF pressure. This is suitable because msl is the IFS model for QFF pressure so the two are interrelated.

## *3.2. MOS Performance Test*

### *3.2.1. Air Temperature*

Figure 3 shows the comparison graph between observation, IFS, and MOS for air temperature. It can be seen that both IFS and MOS can follow the observation fluctuation pattern. However, most of IFS predictions are underestimated. Meanwhile, MOS has more reliable ability because most of the values are not much different from the observation.

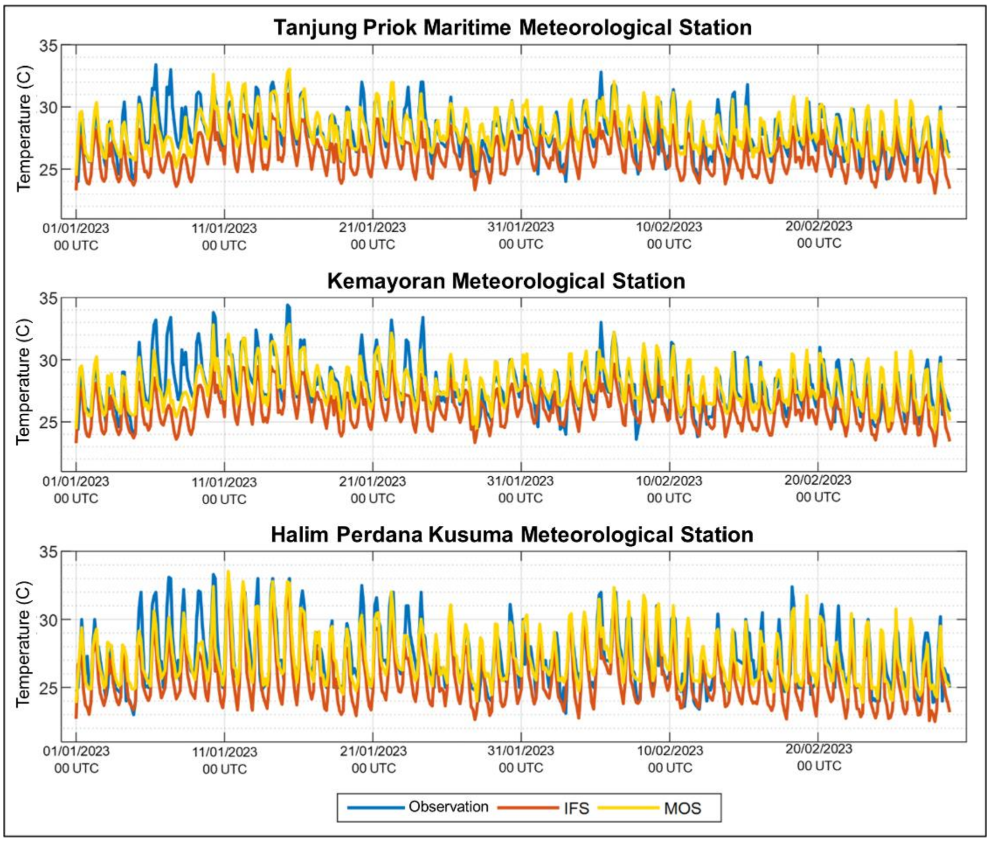


**Figure 3.** Comparison graph between observation, IFS, and MOS for air temperature

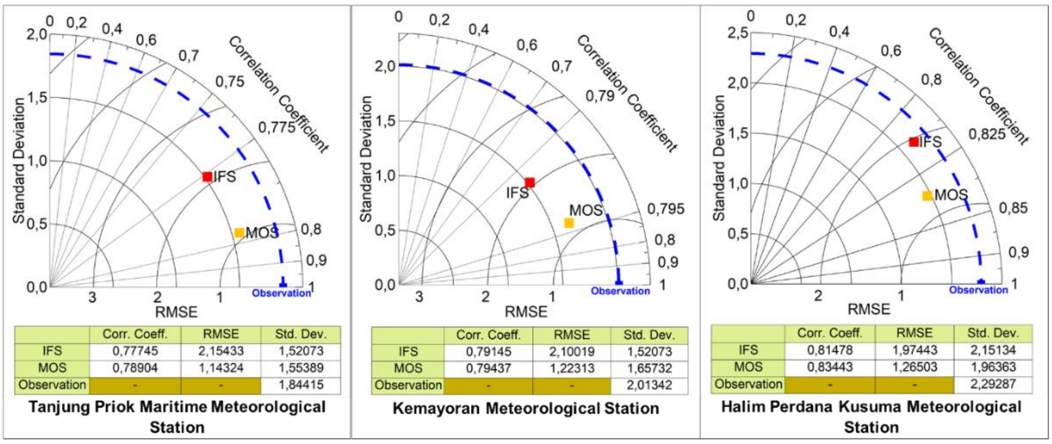


**Figure 4.** Taylor Diagram between observation, IFS, and MOS for air temperature

Taylor diagram in Figure 4 shows that IFS and MOS correlation values are not much different. Based on table 2, the correlation coefficient categories are all in the high relationship category and MOS are always higher than IFS. It means MOS has better relationship with the observation than IFS. The lower RMSE of MOS indicates that MOS tends to produce lower error than IFS. At Tanjung Priok and Kemayoran, standard deviation of observation is closer to MOS than IFS. It explains that the difference distribution between the observed value and the average is better represented by MOS. IFS is not better because the range of deviation is too small. In contrast, at Halim Perdana Kusuma, standard deviation of the observation is more relevant with IFS.

### *3.2.2. Relative Humidity*

Based on figure 5, it appears that both IFS and MOS have similar fluctuation pattern to the observation. However, in some examples, IFS produces zero value that is actually impossible to obtain in observation. IFS also tends to much overestimate compared to MOS. Based on the graph analysis, the ability of MOS to predict humidity is better than IFS.

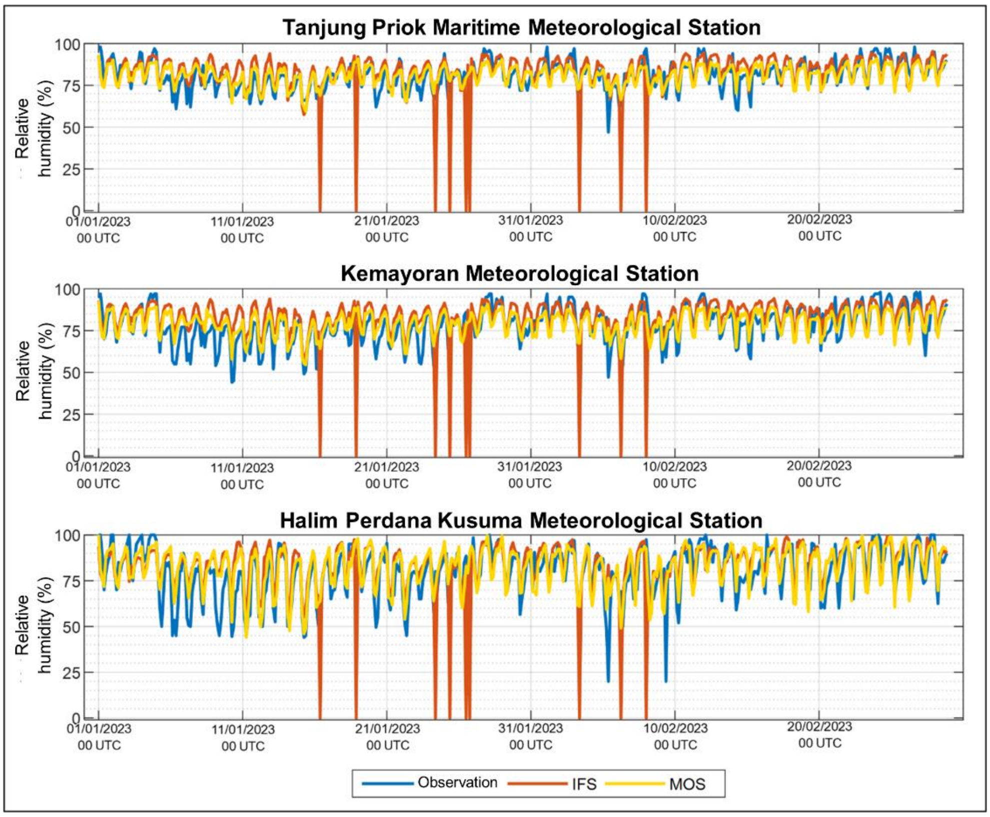


**Figure 5.** Comparison graph between observation, IFS, and MOS for relative humidity

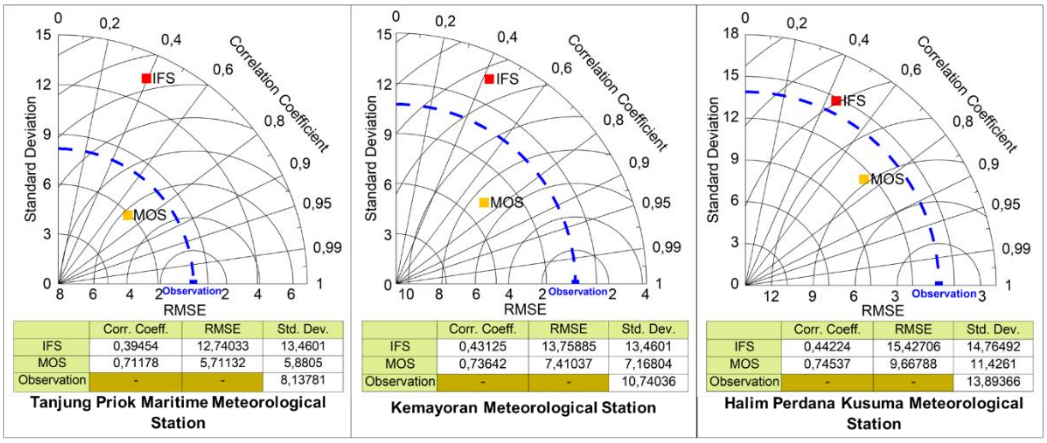


**Figure 6.** Taylor Diagram between observation, IFS, and MOS for relative humidity

Moreover, Taylor diagram in figure 6 shows that the IFS and MOS correlation values are quite far apart. In all three locations, the correlation coefficients of MOS are much higher than IFS. Based on the categories in table 2, MOS correlation coefficients are in the high relationship category. Meanwhile, IFS correlation coefficients are in the category of existing but low relationship (Tanjung Priok Maritime Meteorological Station) and moderate relationship (Kemayoran Meteorological Station and Halim Perdana Kusuma Meteorological Station). In terms of RMSE, MOS are lower so it tends to produce smaller error than IFS. At Tanjung Priok Maritime Meteorological Station, standard deviation of observation is closer to MOS. In contrast, at Kemayoran Meteorological Station and Halim Perdana Kusuma Meteorological Station, the standard deviations of observation are closer to IFS. It means that IFS is not able enough to produce prediction with variance close to the observation.

### *3.2.3. QFF Pressure*

The comparison between observation, IFS, and MOS of QFF Pressure is shown in figure 7. IFS and MOS have similar values and even their graphs seem to overlap. Both are good enough to represent the actual QFF pressure fluctuation. Based on the analysis of the graph, IFS and MOS both have superior performances so it cannot be determined yet which ones are better.

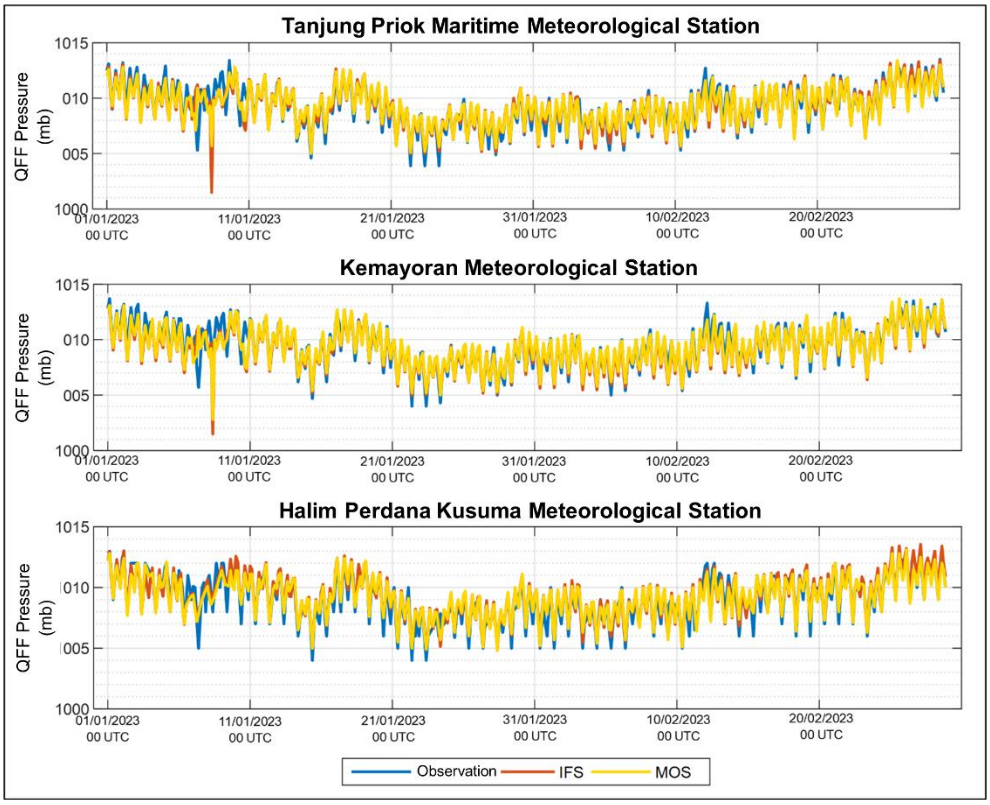


**Figure 7.** Comparison graph between observation, IFS, and MOS for QFF Pressure

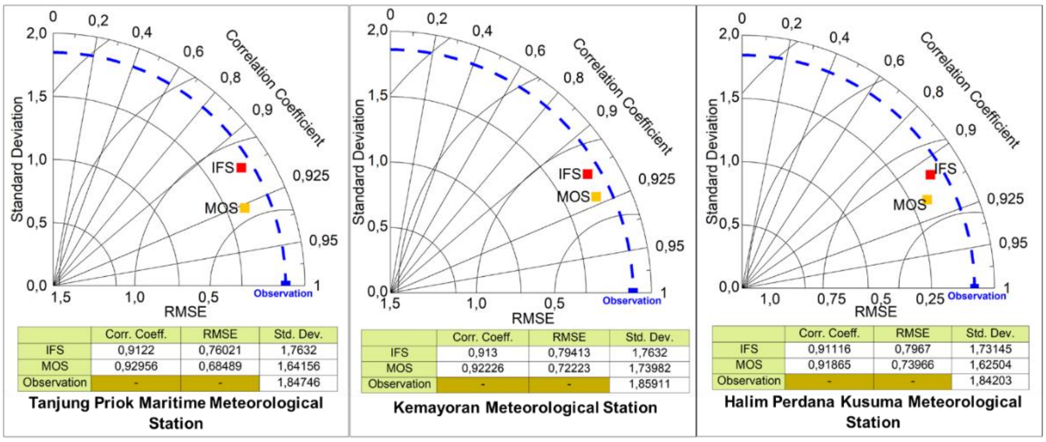


**Figure 8.** Taylor Diagram between observation, IFS, and MOS for QFF Pressure

Based on Taylor diagram in figure 8, MOS has better relationship with observation than IFS, which is characterized by larger correlation coefficient of MOS. In terms of RMSE, MOS tends to produce smaller error than IFS because the RMSE values of MOS are lower. At three locations, the values of observation standard deviation are closer to the IFS standard deviation. It means that MOS is not able enough to produce prediction with variance that is close to the observation.

## 3.3. Cases Test

### 3.3.1. Case of January 1, 2023

Based on figure 9, MOS temperature prediction tends to produce more stable and smoother value than observation. The residual graph also proves that the difference between MOS prediction and observation is between 0 ºC to ±3.4 ºC. When applied in real life, the temperature prediction provides quite suitable result although it is necessary to pay attention to the possibility of residual value.

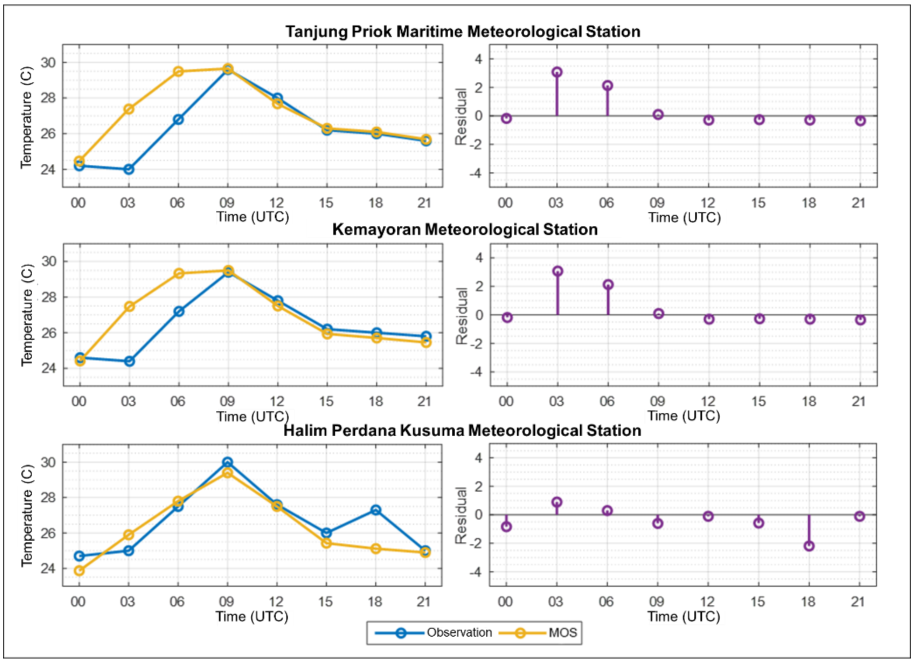


**Figure 9.** Graph of observation and MOS for temperature on January 1, 2023

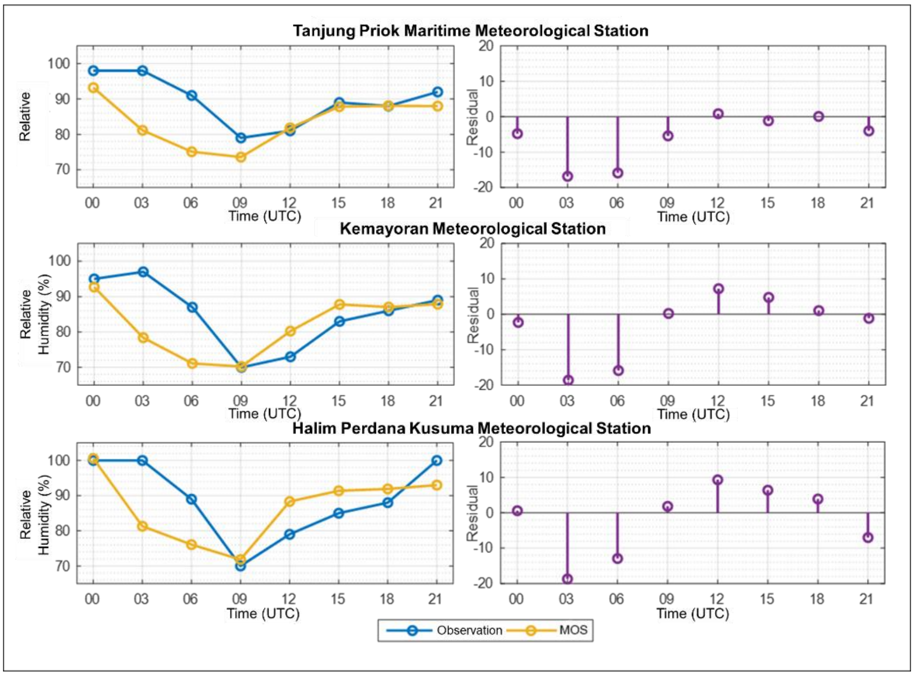


**Figure 10.** Graph of observation and MOS for relative humidity on January 1, 2023

The relative humidity pattern in figure 10 is also quite representative. However, MOS does not provide the precise value because the predicted value tends to be more sloping and smoother. Both lower and higher values potentially overestimate and underestimate. The residual value ranges from 0% to ±19%. MOS is able to predict relative humidity quite well.

Next, QFF pressure result described in figure 11. MOS prediction pattern is quite precise to observation. The graphs appear to almost overlap which means that the values are not much different. The residual value is the lowest among the other two cases, from 0 mb to ±0.6 mb. The application of the MOS prediction for QFF pressure in this case is considered quite appropriate. However, it should be noted that differences within this range remain crucial for aviation meteorology.

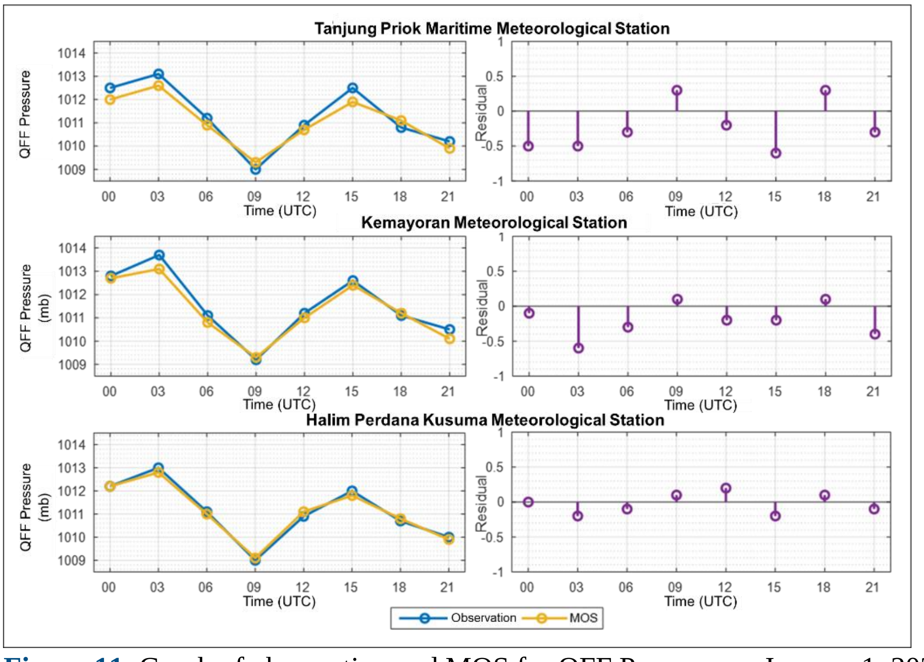


**Figure 11.** Graph of observation and MOS for QFF Pressure on January 1, 2023

## *3.3.2. Case of January 4, 2023*

Based on figure 12, MOS tends to produce temperature value that is more sloping and smoother than observation. The residual graph also proves that the difference between MOS prediction and observation is between 0 ºC to ±3.3 ºC, the lowest of the two cases. When applied in real life, the temperature prediction is quite appropriate, although considering the possible residual value.

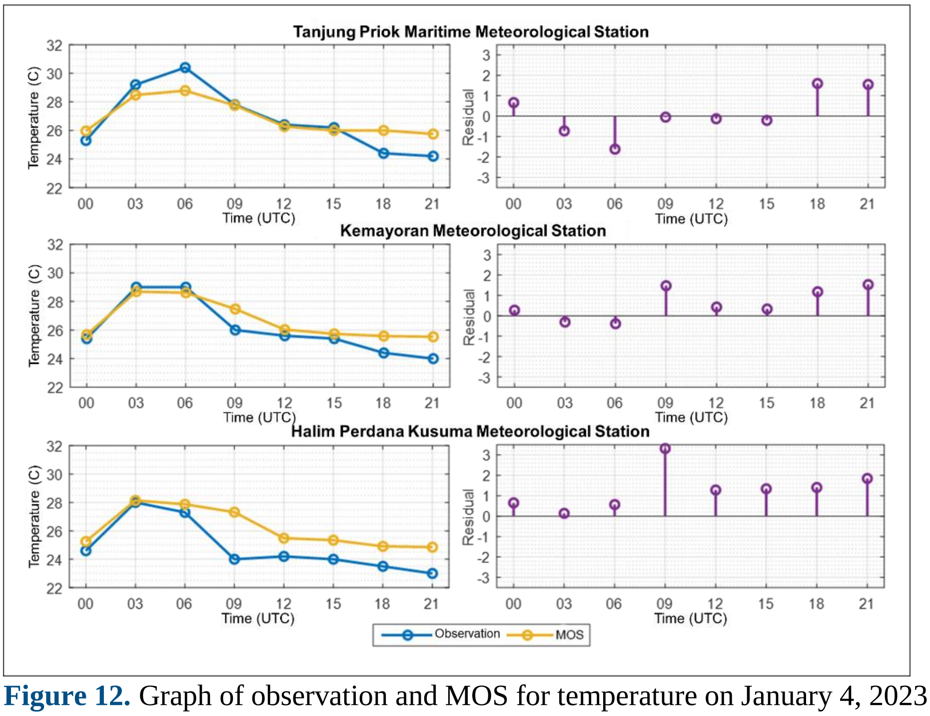


**Figure 12.** Graph of observation and MOS for temperature on January 4, 2023

. Relative humidity pattern that is described by figure 13 is also quite representative. However, MOS is not able enough to provide the right value because the prediction value tends to be sloping. This case has the lowest residual, which the value between 0% and ±9%. MOS is able to predict the relative humidity quite well.

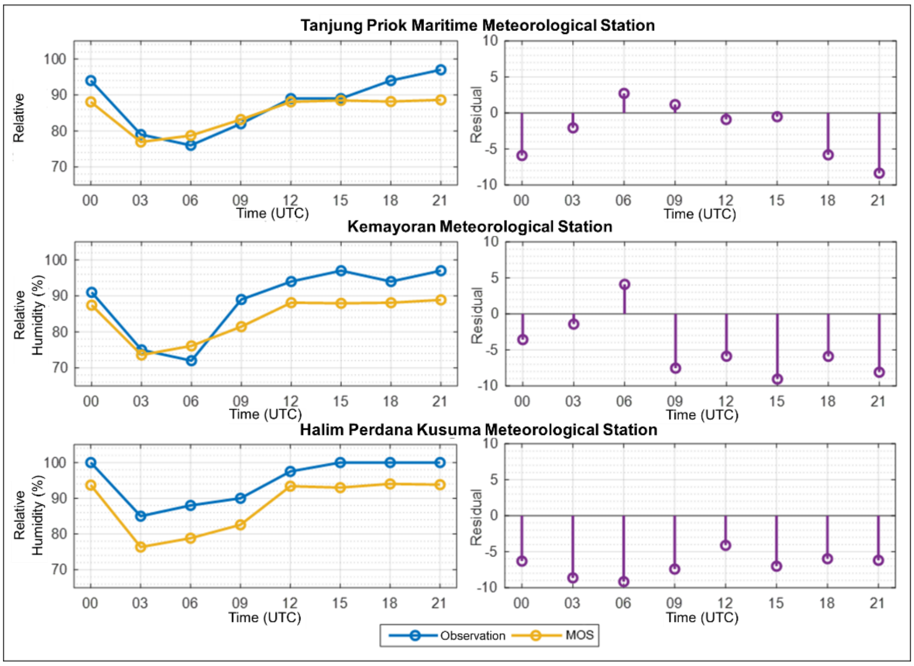


**Figure 13.** Graph of observation and MOS for relative humidity on January 4, 2023

Next, there is QFF pressure which is described in figure 14. MOS prediction pattern is quite consistent with the observation. The graphs appear to almost overlap, which means that the values are not much different. The residual value ranges from 0 mb to ±1 mb. The application of MOS prediction for QFF pressure in this case is considered quite appropriate.

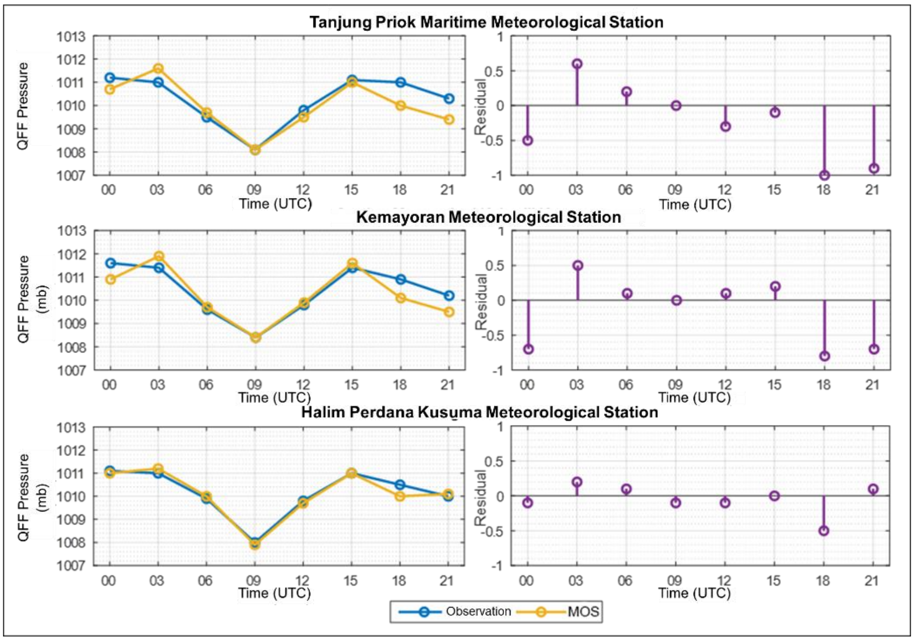


**Figure 14.** Graph of observation and MOS for QFF Pressure on January 4, 2023

### *3.3.3. Case of February 24, 2023*

Based on figure 15, MOS tends to produce temperature value that is more sloping and smoother than observation. The residual graph also proves that the difference between MOS prediction and observation is between 0 ºC to ±3.5 ºC, the highest among the other two cases. When applied in real life, the temperature prediction is quite suitable although it is necessary to pay attention to the possible residual value.

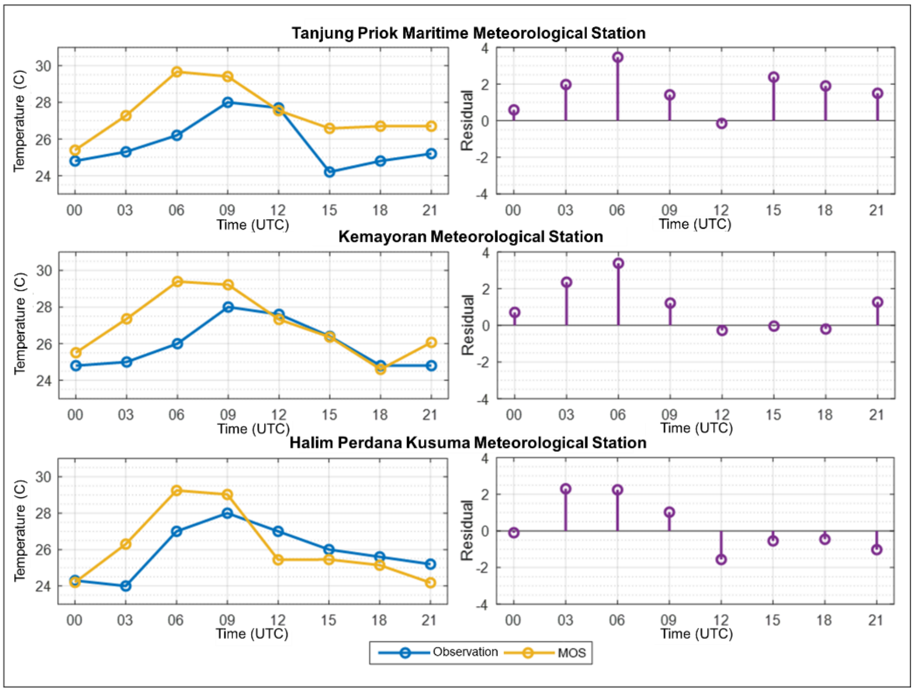


**Figure 15.** Graph of observation and MOS for temperature on February 24, 2023

The relative humidity that is described by figure 16 is also quite representative in pattern. However, MOS does not provide the right value because the prediction value tends to be stable. The residual value ranges from 0% to ±25%, the highest among the other two cases. The MOS prediction result is quite appropriate although it is necessary to pay attention to the possible deviation.

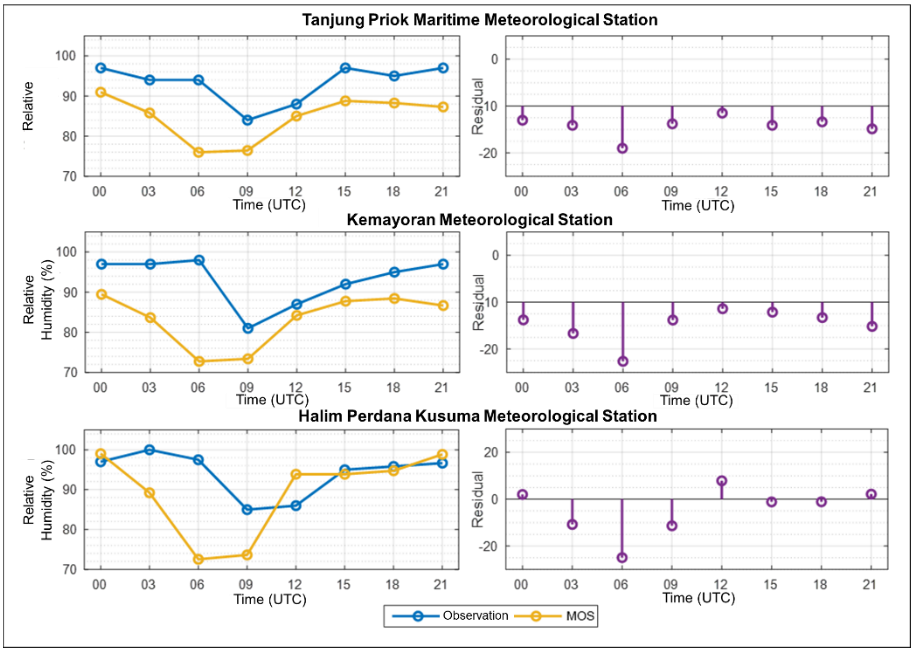


**Figure 16.** Graph of observation and MOS for relative humidity on February 24, 2023

Next, figure 17 describes QFF parameter result. MOS prediction gives a pattern that is quite consistent with observation. The graphs appear to almost overlap which means that the values are not much different. This case has residual value between 0 mb to ±1 mb just like the case of January 4, 2023. The application of MOS prediction for QFF pressure in this case is considered quite appropriate.

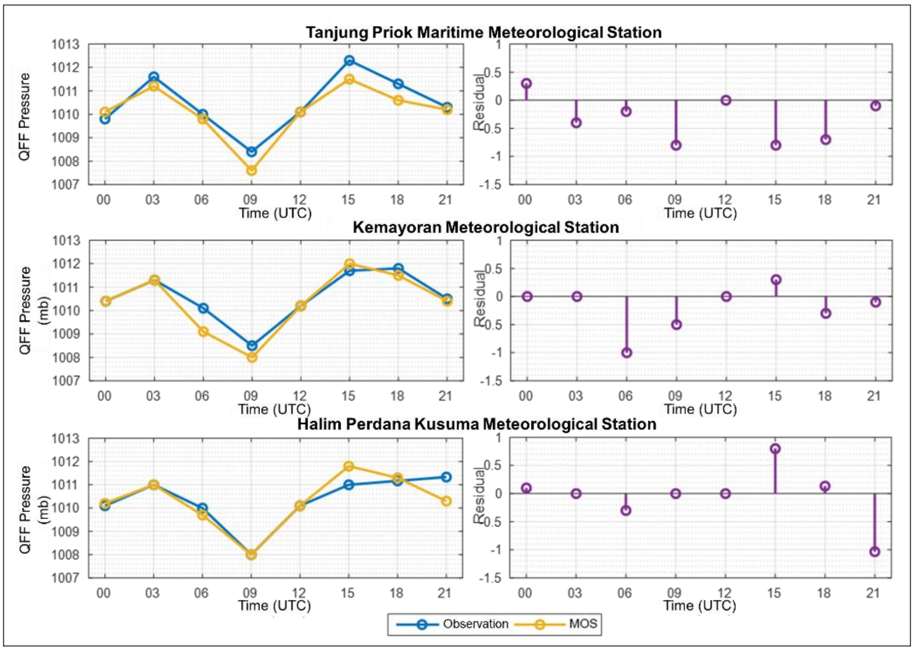


**Figure 17.** Graph of observation and MOS for QFF Pressure on February 24, 2023

## 4. Conclusion

Based on the explanation of the research within the section of results and discussion, the conclusions are as follows.

1. Stepwise regression produces MOS regression model containing the influential parameters for prediction based on the p-value with the highest correlation coefficient. The most influential parameter for temperature is parameter 2t because it is a model of the temperature measurement itself. Relative humidity is most influenced by 2t because temperature and relative humidity is directly proportional. Meanwhile, msl is the most influential parameter for QFF pressure prediction because it is a model of the measurement itself.
2. The MOS performance test generally has superior result and is able to improve the accuracy of IFS prediction. Based on the graphs, MOS prediction results are closer to observation than IFS. Verification of the correlation coefficient and RMSE proves that MOS has higher closeness relationship and lower error rate. However, the standard deviation of MOS for most parameters is not better than IFS. It is because MOS prediction result tends to be more stable with narrower range of value.
3. The result of the heavy rain cases test show that the application of MOS is able to provide fairly accurate prediction while still considering the residual value. The highest residual for temperature is ±3.5 oC, relative humidity is ±25%, and QFF pressure is ±1 mb.

Moreover, there are several suggestions that can be applied to further research, including:

1. Updating data regularly to get the most suitable regression equation and MOS prediction result.
2. Conducting trial on cases with different locations and times to prove the accuracy of MOS prediction.

## Ethics approval

Not required

## Acknowledgments

We would like to express our heartfelt thanks to everyone who contributed to this research. We are especially grateful to Pusat Meteorologi Publik Badan Meteorologi Klimatologi dan Geofisika (BMKG), Tanjung Priok Maritime Meteorological Station, Kemayoran Meteorological Station, and Halim Perdana Kusuma Meteorological Station for supplying the crucial data necessary for this study.

Our appreciation also extends to the reviewers and proofreaders for their thorough work and insightful feedback, which have greatly improved the quality of this publication.

## Competing interests

All the authors declare that there are no conflicts of interest.

## Funding

This study received no external funding.

## Underlying data

Derived data supporting the findings of this study are available from the corresponding author on request.

## Credit Authorship

**Isnaini Ramadhan:** Conceptualization, Methodology, Validation, Formal Analysis, Writing – Original Draft, Visualization. **Deni Septiadi:** Supervision, Writing- Reviewing and Editing.

## References

[1] Badan Nasional Penanggulangan Bencana, "Infografis Bencana Tahun 2022," ["Disaster Infographic 2022"], *Badan Nasional Penanggulangan Bencana*, 2023, [Online]. Available: https://www.bnpb.go.id/infografis/infografis-bencana-tahun-2022. [Accessed: Mar. 7, 2023].

[2] S. Rahmstorf and D. Coumou, "Increase of extreme events in a warming world," In Proc. National Academy of Sciences, 2011, pp. 17905–17909.

[3] Kiki and F. Alam, "Verifikasi parameter presipitasi akumulasi 24 jam pada model cuaca numerik tahun 2017—2020," ["Verification of 24-hour accumulated precipitation on numerical weather prediction model year 2017—2020"], *Megasains*, no. 12, vol. 2, pp. 11—16, Aug. 2021.

[4] J. A. Garcia-Moya, J. L. Casado, I. Martínez, A. Manzao, A. Martín, C. Fernández-Peruchena, M. Gastón. "Deterministic and probabilistic weather forecasting," Agencia Estatal de Meteorología, Spain, Report PREFLEXMS_DEL_D4.3_20160531_v4, 30 Jul. 2016.

[5] H. R. Glahn and D. A. Lowry, "The use of model output statistics (MOS) in objective weather forecasting," *Journal of Applied Meteorology and Climatology*, vol. 11, no. 8, pp. 1203—1211, Dec. 1972.

[6] Nurhayati, "Model output statistic dengan CART dan random forest untuk prakiraan curah hujan harian," ["Model output statistics in daily rainfall forecasting with CART and random forest"], B. S. thesis, Institut Teknologi Sepuluh November, Surabaya, 2017.

[7] N. Brunet, R. Verret, and N. Yacowar, "An objective comparison of model output statistics and "perfect prog" systems in producing numerical weather element forecasts," *Weather and Forecasting*, vol. 3, no. 4, pp. 273—283, Dec. 1988.

[8] Deutscher Wetterdienst, "Model Output Statistics-MIX (MOSMIX)," *Deutscher Wetterdienst: Wetter und Klima aus einer Hand*, 2015, [Online]. Available: https://www.dwd.de/EN/ourservices/met_application_mosmix/met_application_mosmix.html. [Accessed: Apr. 7, 2024].

[9] N. Qona'ah, H. Pratiwi, and Y. Susanti, "Model output statistic dengan principal component regression, partial least square regression, dan ridge regression untuk kalibrasi prakiraan cuaca jangka pendek" ["Model output statistics with principal component regression, partial least square regression, and ridge regression in short-term weather forecast callibration"], *Jurnal Matematika UNAND*, vol. 10, no. 3, pp. 355—368, Jul. 2021.

[10] R. Safitri and Sutikno, "Model output statistics dengan projection pursuit regression untuk meramalkan suhu minimum, suhu maksimum, dan kelembapan" ["Model output statistics with

projection pursuit regression to minimum temperature, maximum temperature, and humidity prediction"], *Jurnal Sains dan Seni ITS*, vol. 1, no. 1, pp. 296–301, Sep. 2012.

[11] J. R. Bocchieri, R. L. Crisci, H. R. Glahn, F. Lewis, and F. T. Globokar, "Recent developments in automated prediction of ceiling and visibility," *Journal of Applied Meteorology*, vol. 13, no. 2, pp. 277—288, Mar. 1974.

[12] W. H. Klein and H. R. Glahn, "Forecasting local weather by means of model output statistics," *Bulletin of the American Meteorological Society*, vol. 55, no. 10, pp. 1217—1227, Oct. 1974.

[13] R. J. Kuligowski and A. P. Barros, "Localized precipitation forecasts from a numerical weather prediction model using artificial neural networks," *Weather and Forecasting*, vol. 13, no. 4, pp. 1194—1204, Dec. 1998.

[14] Badan Penanggulangan Bencana Daerah DKI Jakarta, "Infografis Kejadian Bencana Provinsi DKI Jakarta Tahun 2021," ["Disaster Infographic in DKI Jakarta Province Year 2021"], *Badan Penanggulangan Bencana Daerah DKI Jakarta*, 2022, [Online]. Available: https://bpbd.jakarta.go.id/infografis/30/hasil-rekapitulasi-kejadian-bencana-yang-ada-di-dki-jakarta-pada-tahun. [Accessed: Mar. 3, 2023].

[15] Badan Pusat Statistik Jakarta, "Jumlah Penduduk Menurut Kabupaten/Kota di Provinsi DKI Jakarta (Jiwa), 2020-2022," ["Number of Population by Regency/Municipality in DKI Jakarta Province, 2020-2022"], *Badan Pusat Statistik Jakarta*, 2021, [Online]. Available: https://jakarta.bps.go.id/indicator/12/1270/1/jumlah-penduduk-menurut-kabupaten-kota-di-provinsi-dki-jakarta-.html. [Accessed: Mar. 1, 2023].

[16] J. R. Holton and G. J. Hakim, "An *Introduction to Dynamic Meteorology*, 5th ed., Amsterdam, Netherlands: Academic Press, 2013.

[17] V. Bjerknes, "The problem of weather prediction, considered from the view points of mechanics and physics," *Meteorologische Zeitschrift*, vol. 18, no.6, pp. 663—667, Dec. 2009.

[18] T. N. Palmer, "Predictability of weather and climate: from theory to practice - from days to decades," In Proc. ECMWF Workshop on the Use of High Performance Computers in Meteorology '10, 2003, pp. 1—29.

[19] J. Flemming, V. Huijnen, J. Arteta, P. Bechtold, A. Beljaars, A. M. Blechschmidt, M. Diamantakis, R. J. Engelen, A. Gaudel, A. Inness, L. Jones, B. Josse, E. Katragkou, V. Marecal, V. H. Peuch, A. Richter, M. G. Schultz, O. Stein, and A. Tsikerdekis, "Tropospheric chemistry in the integrated forecasting system of ECMWF." *Geoscientific Model Development*, vol. 8, no. 4, pp. 975—1003, Apr. 2015.

[20] N. Wedi, P. Bauer, W. Deconinck, M. Diamantakis, M. Hamrud, C. Kuehnlein, S. Malardel, K. Mogensen, G. Mozdzynski, and P. Smolarkiewicz, "The modelling infrastructure of the integrated forecasting system: recent advances and future challenges," European Centre for Medium-Range Weather Forecasts, Reading, UK, Tech. Memorandum. 760, Nov. 2015.

[21] F. M. Lopes, R. Conceição, H. G. Silva, T. Fasquelle, R. Salgado, P. Canhoto, and M. Collares-Pereira, "Short-term forecasts of dni from an integrated forecasting system (ECMWF) for optimized operational strategies of a central receiver system," *Energies*, vol. 12, no. 7, pp. 1—18, Apr. 2019.

[22] European Centre for Medium-Range Weather Forecasts, "ECMWF IFS CY41r2 High-Resolution Operational Forecasts," *UCAR/NCAR - Research Data Archive*, 2016, [Online]. Available: http://rda.ucar.edu/datasets/ds113.1/. [Accessed: Feb. 15, 2023].

[23] European Centre for Medium-Range Weather Forecasts, "Operational Configurations of the ECMWF Integrated Forecasting System (IFS)," *UCAR/NCAR - Research Data Archive*, 2016, [Online]. Available: https://confluence.ecmwf.int/pages/viewpage.action?pageId=324860211. [Accessed: Feb. 15, 2023].

[24] G. E. P. Box, G. M. Jenkins, G. C. Reinsel, G. M. Ljung. *Time Series Analysis: Forecasting and Control*, 5th ed., Hoboken, NJ: Wiley, 2015.